Phylogenetic signal analysis in the basicranium of Ursidae (Carnivora, Mammalia)

María Eugenia Arnaudo[1,2], Néstor Toledo[2,3], Leopoldo Soibelzon[2,4] and Paula Bona[2,3]

[1] División de Paleontología Vertebrados, Facultad de Ciencias Naturales y Museo-UNLP, La Plata, Buenos Aires, Argentina
[2] CONICET, Consejo Nacional de Investigaciones Científicas y Técnicas, Buenos Aires, Argentina
[3] División Paleontología Vertebrados, Unidades de Investigación Anexo Museo, Facultad de Ciencias Naturales y Museo-UNLP, La Plata, Buenos Aires, Argentina
[4] Laboratorio de Morfología Evolutiva y Desarrollo (MORPHOS)-División de Paleontología Vertebrados, Facultad de Ciencias Naturales y Museo-UNLP, La Plata, Buenos Aires, Argentina

Corresponding author
María Eugenia Arnaudo,
mearnaudo@gmail.com

ABSTRACT

Ursidae is a monophyletic group comprised of three subfamilies: Tremarctinae, Ursinae and Ailuropodinae, all of which have a rich geographical distribution. The phylogenetic relationships within the Ursidae group have been underexamined, especially regarding morphological traits such as the basicranium. Importantly, the basicranium is a highly complex region that covers a small portion of the skull, combining both structural and functional aspects that determine its morphology. Phylogenetic hypotheses of the Ursidae (including Tremarctinae) have been made based on morphological characters that considers skull, mandible and teeth features, while specific characters of the auditory region and basicranium have not been taken into account. To do this, we analyse the shape and size macroevolution of the basicranium of Ursidae, testing its morphological disparity in a phylogenetic context, which is quantified by means of the phylogenetic signal. We investigated phylogenetical autocorrelation by shape (depicted by Principal Components Analysis scores from previous published analyses) and basicranium size (depicted by centroid size, CS) using an orthonormal decomposition analysis and Abouheif C mean. The main advantages of these methods are that they rely exclusively on cladogram topology and do not require branch-length estimates. Also, an optimisation of the ancestral nodes was performed using TNT 1.5 software. In relation to the phylogenetic signal, both methods showed similar results: the presence of autocorrelation was detected in PC1 and PC2, while in PC3, PC4 and PC5 and in the size of the basicranium (CS), the absence of autocorrelation occurred. The most significant nodes (where there is autocorrelation) are the basal nodes 'Ursidae' and 'Ursinae-Tremarctinae'. Within this last group, distinctive basicranium morphology is observed, being more conservative in Tremarctinae than in Ursinae. The differences between these subfamilies could be related to historical events involving varying food and environmental preferences. The high phylogenetic signal in the node Tremarctinae probably indicates that the basicranium configuration of these bears was obtained early in their evolutionary history. Finally, our results of the basicranium and skull length ratios indicate that in Tremarctinae, the basicranium size was not determined by phylogeny but instead by other factors, such as adaptive responses to climatic changes and competition with other carnivores.

INTRODUCTION

Ursidae is a monophyletic group of placental carnivoran mammals comprised of three subfamilies: Ursinae, Ailuropodinae and Tremactinae. The family has been found in America, Asia, Europe, Africa and India from the late Paleogene to recent times.

Within Ursinae, three extant genera are recognised, encompassing the following species: the American black bear *Ursus americanus*, the brown bear *U. arctos*, the polar bear *U. maritimus*, the Asian black bear *U. thibetanus*, the sloth bear *Melursus ursinus,* the sun bear *Helarctos malayanus* and several fossil representatives (*Wilson & Reeder, 2005*; *Garshelis, 2009*). This subfamily is distributed throughout Eurasia, North America and—in the past—in the Atlas Mountains of North Africa (*Garshelis, 2009*) since the early Miocene period up to recent times (*Krause et al., 2008*).

The Ailuropodinae includes just one living species, the giant panda *Ailuropoda melanoleuca*, which is distributed in the mountains of the central region of China. Although its systematics have been a matter of debate, it is currently considered a member of Ursidae (*O'Brien et al., 1985*; *Krause et al., 2008*; *Juárez Casillas & Varas, 2011*). The oldest record of this subfamily corresponds to the late Pliocene of China and the Asian Southeast (*Jin et al., 2007*).

Tremarctinae is comprised of four genera: *Plionarctos*; *Arctodus*; *Arctotherium* and *Tremarctos*. *Plionartos* is comprised of *P. edenensis* and *P. harroldorum*; *Arctodus* contains *A r . pristinus* and *A r . simus*; within *Arctotherium* are the following species: *A. angustidens*, *A. vetustum*, *A. bonariense*, *A. tarijense* and *A. wingei*; and finally *Tremarctos* includes *T. floridanus* and the extant spectacled bear *T. ornatus*, being the latest species of the only extant Tremarctinae (*Soibelzon, 2002*; *Soibelzon, 2004*). This subfamily is distributed exclusively in America, from Alaska to the southern region of Chile; it was first recorded in the late Miocene in North America (*Soibelzon, Tonni & Bond, 2005*).

The basicranium in mammals is a complex region that forms the floor of the brain case (a relatively small portion of the ventral surface of the skull). In mammals, the brain fills the cerebral cavity by up to 95% (*Jerison, 1973*), so the morphology and dimensions of the brain case gives an approximation of the shape and relative size of the encephalon and main sensitive organs contained within there. The basicranium presents neurovascular foramina for the passage of several cranial nerves (i.e., CNs XII-IX, the mandibular branch of the trigeminous nerve, the cordae tympani nerve, the facial nerve VII, the auricular branch of vagus nerve, etc.) veins and arteries (i.e., the internal jugular vein, the internal carotid artery and veins from the transverse and inferior petrosal sinuses, the internal facial vein, stylomastoid artery, etc.) and the opening of the Eustachian tubes. Other bony landmarks such as muscular attachments and other anatomical structures (e.g., outline and relative size of the tympanic, hyojugular fossa) are often used in comparative anatomical studies and are related to several biological functions such as mastication, balance and audition,

among others (e.g., *Davis, 1964*; *Wible, 1986*; *Wible, 1987*; *Wozencraft, 1989*; *Lieberman, Ross & Ravosa, 2000*; *Strait, 2001*). Despite some authors previously considering that the basicranium is morphologically conservative (e.g., *Turner, 1848*), it is an element of potential importance in phylogeny and hence in the evolutionary history of carnivores specifically and in mammals generally (*Mitchell & Tedford, 1973*; *Radinsky, 1969*; *Radinsky, 1971*; *Radinsky, 1973*; *Radinsky, 1974*; *Neff, 1987*; *Wozencraft, 1989*; *Wible & Hopson, 1993*; *Wang & Tedford, 1994*; *Lieberman, Ross & Ravosa, 2000*; *Hunt, 2001*).

Given that the braincase and basicranium reflect the morphology of the encephalon and sense organs, a study of the basicranium can provide inferences related to a mammal's behaviour. This is particularly relevant in paleobiological analyses, when fossil specimens preserve only fragments of the brain case and when no data of the postcranium or cranio-dental traits can be recovered.

Similar to what occurs with other parts of the skeleton, the morphological variation of the brain case can be explained by a combination of phylogenetic history and autapomorphic adaptations to different life habits, as well as the animal's ability to move and feed. In this sense, an interesting approach for interpreting the morphological variation within a lineage is the analysis of the life history traits of taxa expressed as quantitative variables in a phylogenetic context (*Ollier, Couteron & Chessell, 2006*). When close relatives in a phylogeny are more similar than distant relatives, the morphological pattern observed presents a phylogenetic signal (*Harvey & Pagel, 1991*). Species' traits can show a high or low phylogenetic signal; when the phylogenetic signal is high, closely related species exhibit similar trait values, and trait similarity decreases as phylogenetic distance increases (*Losos, 2008*). Conversely, a trait that shows a weak phylogenetic signal may vary randomly across a phylogeny, and distantly related species often converge on a similar trait value, while closely related species exhibit notably different trait values (*Kamilar & Muldoon, 2010*; *Kamilar & Cooper, 2013*).

The morphological disparity of the basicranium of Ursidae has often been discussed (e.g., *Torres, 1988*; *García et al., 2007*; *Rabeder, Pacher & Withalm, 2010*; *Santos et al., 2014*; *Koufos, Konidaris & Harvati, 2017*; *Arnaudo & Fernandez Blanco, 2016*), but almost all of these studies have focused on ursine bears (e.g., *Ursus spelaeus*, *U. deningeri*). The phylogenetic hypotheses of the Ursidae (including Tremarctinae) have been made based on morphological characters that consider skull, mandible and teeth features using a molecular analysis; however, the specific characteristics of the auditory region and basicranium have not been taken into account (e.g., *Trajano & Ferrarezzi, 1994*; *Ubilla & Perea, 1999*; *Soibelzon, 2002*; *Pagès et al., 2008*; *Soibelzon, Schubert & Posadas, 2010*; *Kumar et al., 2017*).

The aim of the current work is to analyse the macroevolution of the shape and size of the braincase of Ursidae, testing its morphological variations in a phylogenetic context. To accomplish this, we used previous results published by *Arnaudo & Fernandez Blanco (2016)*, who studied the auditory region and basicranium of Ursidae using a two-dimensional geometric morphometric approach (see the supplementary material for further explanation). *Arnaudo & Fernandez Blanco (2016)* found that the main groups of bears (i.e., subfamilies) can be clustered by the shape of the basicranium and auditory

region, and the authors concluded that the disparity of that part of the brain case could be explained by the phylogenetic history of the clade.

MATERIALS AND METHODS

The cranium of Ursidae was analysed from a sample of 164 extinct and extant species, as listed in Table S1. The morphological variation of the basicranium was considered using the PC scores reported by *Arnaudo & Fernandez Blanco (2016)*, which were based on two-dimensional geometric morphometric (Table S2 and also see the summary of the results from (*Arnaudo & Fernandez Blanco, 2016*) in the supplementary material for further explanation).

Because of the lack of available phylogenetic hypotheses, including the fossils of ursids (especially tremarctines), a super tree was built from two different sources using the Mesquite software package (*Maddison & Maddison, 2017*). For extant species, the phylogeny taken into account was proposed by *Krause et al. (2008)*, and this was based on molecular data. An extended approach to build more complete phylogenies is to assemble super trees by combining these backbone phylogenies with smaller, overlapping trees (*Bininda-Emonds, 2004*; *Baker et al., 2009*). Because of this, super trees usually lack accurate branch-length information, or branch-length data can even be missing (i.e., the resultant super trees only provide topological information; (*Molina-Venegas 2017*).

Two different phylogenetic hypotheses were compared. The first—cladogram A (*Mitchell et al., 2016*)—is based on molecular data and takes *Arctodus* as a sister taxon of the clade formed by *Arctotherium + Tremarctos* (Fig. 1).

The second hypothesis—cladogram B (*Soibelzon, 2002*)—is based on morphological data and considers the spectacled bear clade (*Tremarctos floridanus* and *T. ornatus*) to be the sister group of the short-faced bear clade (which includes *Arctodus* and *Arctotherium*; Fig. S1).

Phylogenetical autocorrelation—Orthonormal decomposition and Abouheif's C mean methods

We performed analyses to search for phylogenetical autocorrelations in shape and size (depicted by centroid size, CS; *Hood, 2000*). As described in *Arnaudo & Fernandez Blanco (2016)*, major shape variations were a focus in the first and second Principal Components (PCs) (PC1 = 48.5% and PC2 = 15.7%), with the explained variance dropping below the 5% beyond the fourth PC (Fig. S2). Thus, we analysed the phylogenetical signal present only in the first five PCs. Because the inference of branch length for the fossil taxa could not be carried out with certainty, we used two tests that did not require estimating the branch lengths, relying exclusively on cladogram topology instead: the orthonormal decomposition (*Ollier, Couteron & Chessell, 2006*) and the Abouheif (*Abouheif, 1999*) analyses. All calculations were performed in the R free statistical suite (*R Core Team, 2018*), employing different tools from the *ade4* (*Dray & Dufour, 2007*), *ape* (*Paradis, Claude & Strimmer, 2004*), *geiger* (*Harmon et al., 2008*), *adephylo* (*Dray & Jombart, 2008*) and *phylosignal* (*Keck et al., 2016*) packages.
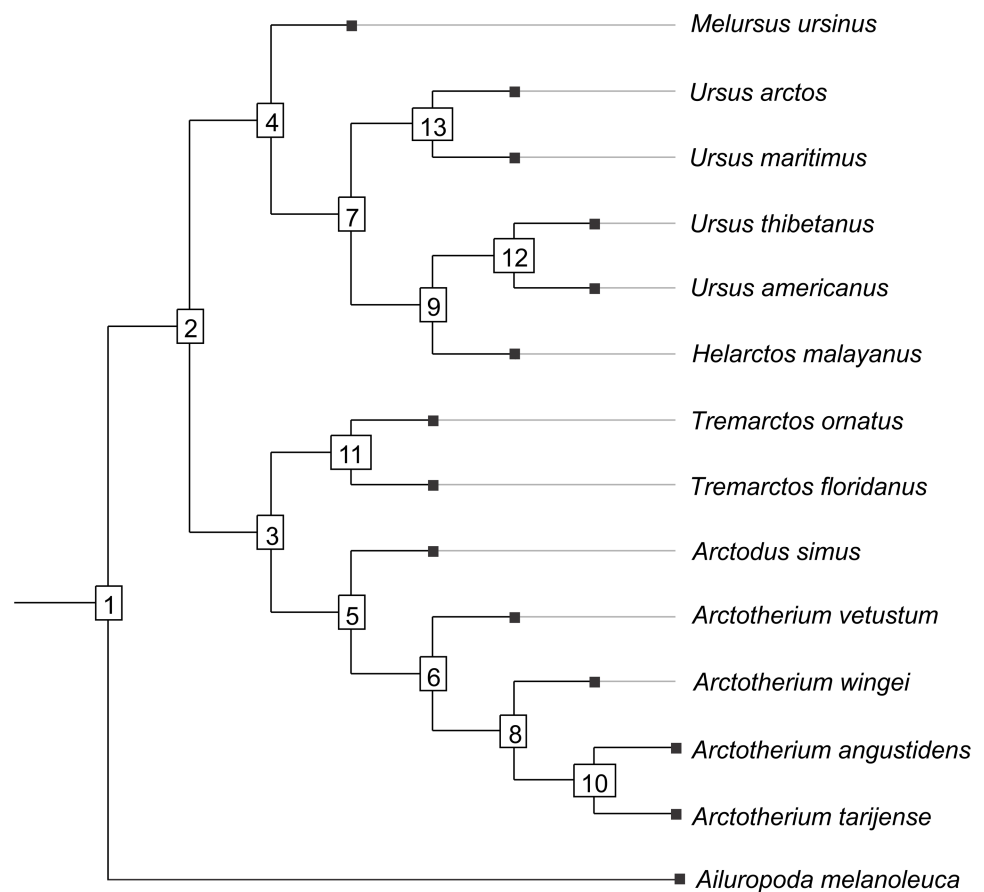
Figure 1 **Cladogram B.** Phylogenetic tree topology of the Cladogram A used in this study for the Ursidae family. The numbers of the clade correspond with the numbers obtained using orthonormal decomposition analysis.

The orthonormal decomposition analysis allows for the detection of specific nodes where autocorrelation is higher. This test (as implemented in the *ade4* package) builds a matrix of orthobases (i.e., orthonormal vectors depicting the topological information of the tree) and then analyses the correlation between the studied variables (PC scores and CS) and each orthobasis vector by means of four nonparametric statistics. The construction of a null model of no-correlation and confidence intervals (at alpha 0.05) for the statistics is achieved by Monte Carlo permutations of the orthobases vector matrix against the studied variables. The R2Max (maximal R2) depicts high values whenever a significant share of dependence is detected at a single node (otherwise, dependence is overspread through several nodes). The Dmax (maximal deviation) corresponds to the Kolmogorov–Smirnov statistic and tests if the studied variable is similar to a random sample from a uniform distribution. The SkR2k (sum of k-nth R2) depicts the skewness toward the tree's tips or roots, that is, the proportion of variance explained by basal nodes versus terminal ones. The sum of cumulative errors (SCE) describes the averaged variation.

Abouheif's C index is considered a special case of spatial correlation index in Moran's I (*Gittleman & Kot, 1990*); it was performed for studying the correlation between the studied variables (PC scores and CS) and a matrix of phylogenetic proximities with a non-null diagonal (see *Pavoine et al., 2008*), which summarises the topology of the cladogram. The calculation of the proximity matrix was performed using the 'oriAbouheif' method of the command *proxTips* (*adephylo* R package), as discussed in *Pavoine et al. (2008)*. Then, this matrix was used as an input for the *gearymoran* function of the *ade4* R package. The null hypothesis is the absence of correlation (the C mean equals 0), and the significance of the observed parameter is tested against a distribution built on permutations.

Landmark optimisation

Optimisation of the ancestral nodes was performed using TNT 1.5 software (*Goloboff & Catalano, 2016*); this version integrates landmark data from TPS files into a phylogenetic analysis. Landmark data consist of coordinates (in two or three dimensions) for the terminal taxa; TNT reconstructs shapes for the internal nodes such that the difference between the ancestor and descendant shapes for all tree branches sums up to a minimum. Then, this sum is used as tree score (*Goloboff & Catalano, 2016*).

Skull proportions

To compare relative changes in the shape of the basicranium with respect to the skull as a whole, a ratio between the anteroposterior length of the basicranium (bsL) and the anteroposterior total length of the skull (stL) is used.

This ratio describes the proportional length of the basicranium compared with the rest of the skull. Measurements were taken on orientated photographs of almost the total sample (some fossil specimens were incomplete, so the total length could not be measured for these) of the ursids using ImageJ software (*Rasband, 2006*). The differences between subfamilies were analysed using nonparametric statistical tests (Kruskal–Wallis and Wilcoxon rank-sum tests). Calculations were performed in R using the *kruskal.test* and *pairwise.wilcox.test* functions of the core package *stats*.

RESULTS

Orthonormal decomposition of variance (Figs. S3–S15)

The results obtained rendered no differences between the phylogenetic hypotheses considered in the current study, so to avoid repetition, we describe the results concerning the cladogram A, which was recently published by *Mitchell et al. (2016)* (for results concerning the cladogram B, see Figs. S5, S7, S9, S11, S13 and S15).

The presence of autocorrelation was detected in PC1 and PC2 (Figs. 2A–2L), while PC3, PC4 and PC5 and the size of the basicranium (CS) did not show any significant differences from the null model of a uniform distribution of the orthogram values (Figs. S10, S12, S14). We infer absence of a phylogenetic signal in CS, PC3, PC4 and PC5 (Figs. S4, S10, S12, S14), because the observed values of the four corresponding statistics were all exceeded by the results of many Monte Carlo randomisations (see *Ollier, Couteron & Chessell, 2006*). Finally, the values of the cumulated orthogram remained within the confidence limits.
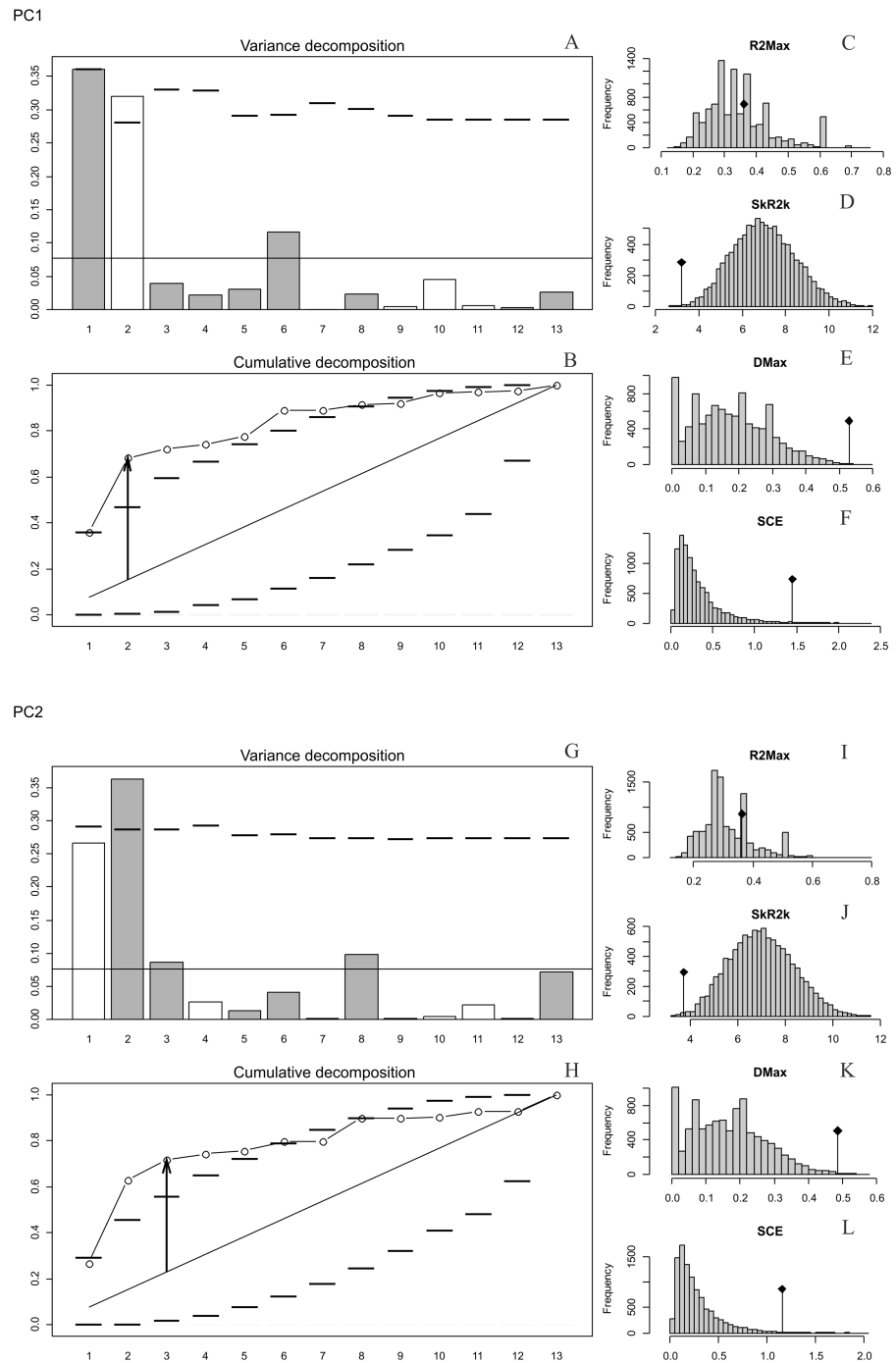
Figure 2 **Orthonormal decomposition results of PC1 and PC2 for Cladogram A.** (A, G) Orthogram plot: height of bars is proportional to the squared coefficients (white and grey bars represents positive and negative coefficients); dashed line is the upper confidence limit at 5%, built from Monte Carlo permutations; horizontal solid line is the mean value; (B, H) Cumulative orthogram plot: circles represent observed values of cumulated squared coefficients (vertical axis); the expected values under H_0 are disposed on the straight line; dashed lines represent the bilateral confidence interval; (C–F; I–L) Histograms of observed values of the four statistic tests: black dot depicts the observed parameter value.

In both PC1 and PC2, the most significant nodes (where there is an autocorrelation) are the basal nodes 'Ursidae' (1) and 'Ursinae-Tremarctinae' (2). In PC1, the nodes '*Ursus +H. malayanus*' (6) and '*U. arctos-U. maritimus*' (10; Fig. 3A), and in PC2, the nodes 'Tremarctinae' (3) and '*U. americanus+U. thibetanus - H. malayanus*' (8) also show a phylogenetic signal (Fig. 3B).

In both PCs, the statistics from R2Max are nonsignificant ($p = 0.37$ for PC1 and $p = 0.28$ for PC2), but significant values were obtained for SkR2k, DMax and SCE (Figs. S6, S8).

In both PCs, a 'diffuse phylogenetic dependence', as defined by *Ollier, Couteron & Chessell (2006)*, is observed to the degree to which the phylogenetic history has shaped the evolution of phenotypic characters or life traits. This is given by the presence of a significant departure from H0 in three test statistics (SkR2k, DMax and SCE, while the cumulative orthogram has several values outside the confidence limits Figs. 2D–2F, 2J–2L) and R2Max statistics, which is nonsignificant (see above; Figs. 2C, 2I). The values of the orthogram—thus the portions of interspecific variance—decrease regularly as a function of the complexity value, np, of the nodes. In PC1 and PC2, the variation of the trait is accumulated mostly at the root of the tree, while in the tips of the tree, the variation decreases. According to the cumulative decomposition plots, in all cases, several nodes show values extending beyond the confidence limits built by the Monte Carlo permutations (Fig. 2).

Abouheif C mean

The observed position of the C mean statistic is significantly different from the expected sampling distribution of the null hypothesis developed by randomising the tips at a 0.05 alpha for PC1 and PC2; therefore, there is a statistically significant autocorrelation (Figs. 4A, 4B). For PC3, PC4, PC5 and size (CS), the observed position of the C mean is not significantly different than the expected sampling distribution of the null hypothesis developed by randomising the tips at a 0.05 alpha. Therefore, phylogeny is not a significant factor for centroid size; but for shape, closely related taxa are more similar than expected (Figs. 4C–4F).

Landmark optimisation

The ancestral configuration of the basicranium was analysed in the nodes that showed a significant phylogenetic signal. The basicranium at the basal node 'Ursidae' (Fig. 5, node 14) was reconstructed as antero-posteriorly short and laterally expanded; the basioccipital–basisphenoid contact was anteriorly convex; the otic region was also reduced, while the mastoid processes were wide; the occipital condyles are more anteriorly located and aligned with the paroccipital processes. This morphology coincides with that of *Ailuropoda melanoleuca.* In the node 'Tremarctinae+Ursinae' (Fig. 5, node 20), the basicranium is more antero-posteriorly expanded; with a straight basioccipital–basisphenoid contact, the otic region is more expanded but with narrower mastoid processes and occipital condyles posteriorly placed with respect to the paraoccipital processes. In the node 'Tremarctinae' (Fig. 5, node 19), the basicranium configuration differs from that of the most inclusive nodes in that it is laterally narrower and antero-posteriorly elongated, differing from that of the
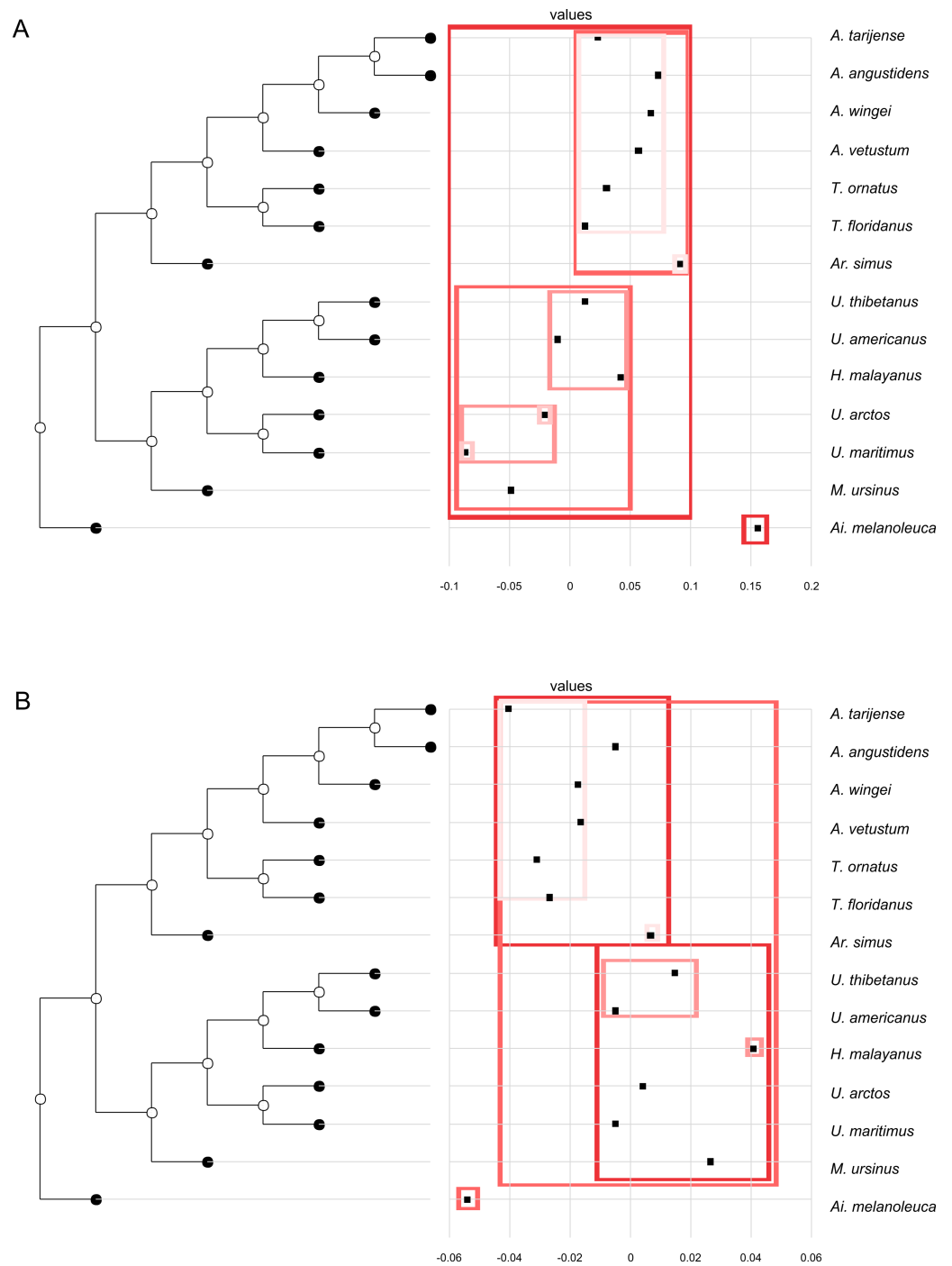
Figure 3 Phylogenetic tree with dotplot of the shape of the basicranium (depicted as PC scores) and species names for PC1 (A) and PC2 (B). Boxes in shades of red enclose variation explained by nodes in decreasing (from red to pink) importance as determined by orthonormal decomposition (see Fig. 4).
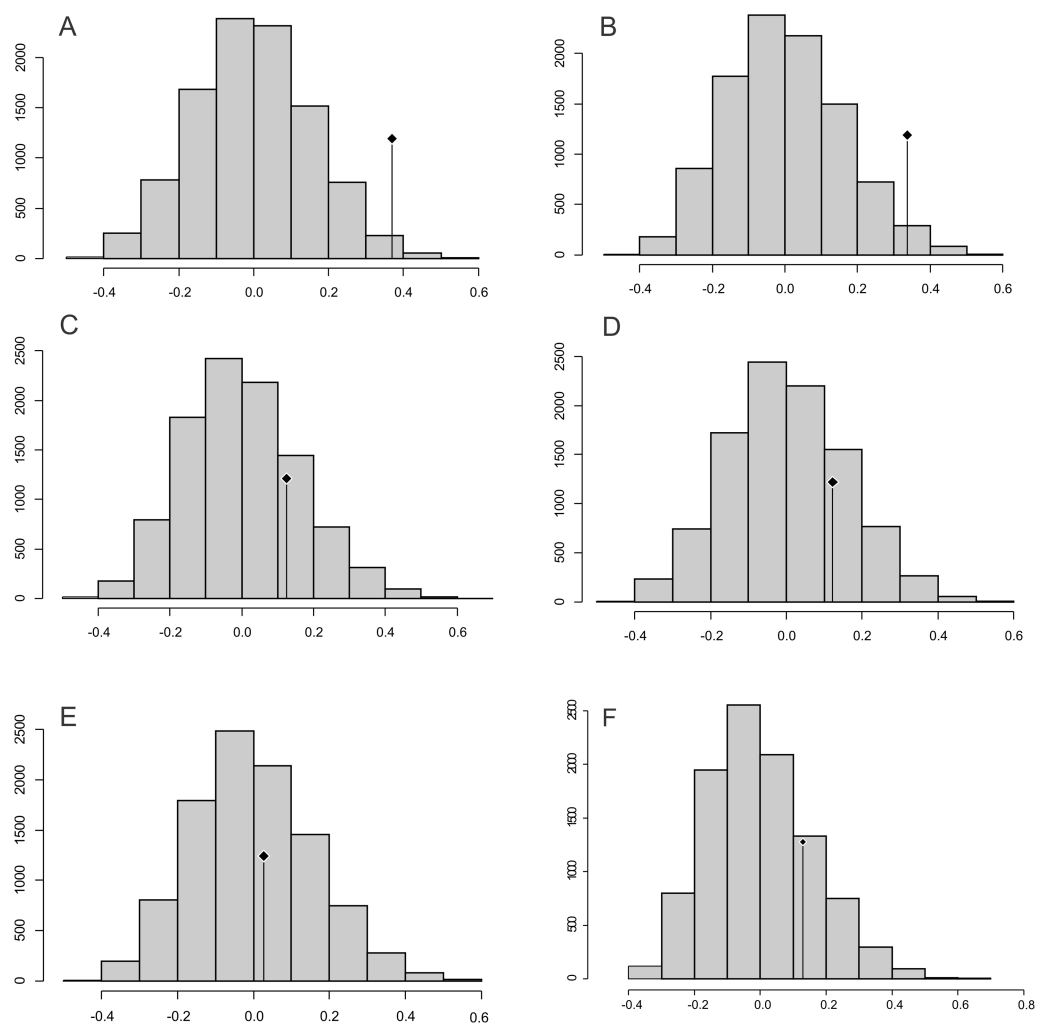
Figure 4 Abouheif C-mean results for the first's five PC (A–E, respectively) axes and the centroid size (F). Black dots indicate the position of the observed C-mean statistic relative to the H_0 hypothesis developed by randomizations along the tips of the phylogeny.

node 'Ursinae' (Fig. 5, node 25) in having a straight basioccipital–basisphenoid contact and an otic region that is more anteriorly placed and slightly expanded but with wider mastoid processes. In the node 'Ursinae', the basicranium is more antero-posteriorly elongated than in more inclusive nodes, and in the node 'Tremarctinae', the basioccipital–basisphenoid contact is anteriorly concave, the mastoid processes are narrower, the occipital condyles are posteriorly located, and the otic region is more expanded with a larger tympanic bone.

Skull proportions

The relative proportions of the basicranium rendered significant differences between subfamilies (Table S3), indicating that the basicranium is comparatively shorter in Ailuropodinae when compared with Tremarctinae and Ursinae and in turn shorter in Tremarctinae than in Ursinae (Fig. 6). Also, a small difference is present in the basicranium
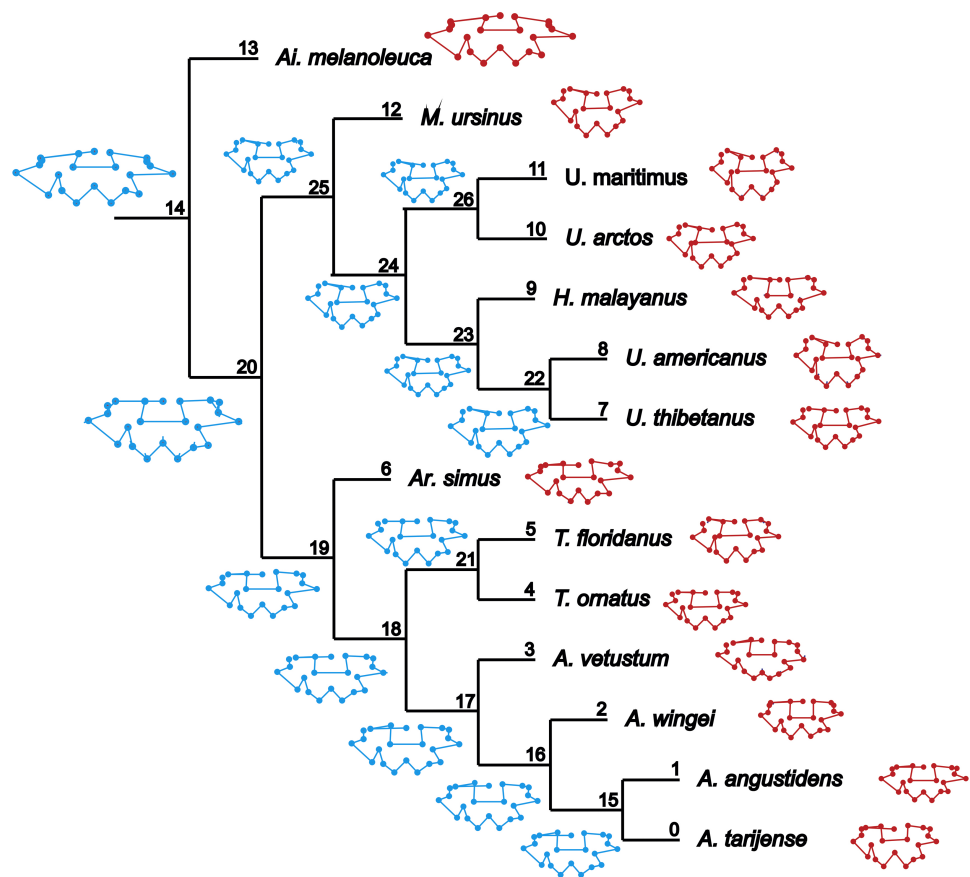
Figure 5 Landmark optimization. Reconstruction of the shape of the basicranium for nodes (in blue) and observed landmark configuration of terminals (in red).

within Tremarctinae (i.e., *A. angustidens* and *Ar. simus* presents a skull ratio of 0.20, while *A. wingei* has a skull ratio of 0.26).

DISCUSSION

According to the morphological variability of the basicranium in ursids, *Arnaudo & Fernandez Blanco (2016)* found that the distribution of taxa in the morphospace results in groups that are fixed with the recognised clades Tremarctinae, Ursinae and Ailuropodinae and that the Ursinae presents a higher disparity at the basicranium than Tremarctinae (Fig. S16). Among ursids, *Ailuropoda melanoleuca* shows a very distinct (which potentially could be plesiomorphic, although this hypothesis must be tested with future inclusion of additional outgroups; Fig. 5) configuration of the basicranium: rectangular, antero-posteriorly shorter and a wider basicranium, with wide processus mastoideus, short occipital condyles antero-posteriorly located, a ventral border of the foramen magnum anteriorly located, and basioccipital–basisphenoid contact anteriorly convex. A more derived morphology could be found in Ursinae (Fig. 5) with a rhomboidal, more antero-posteriorly elongated and narrower basicranium, with the basioccipital–basisphenoid
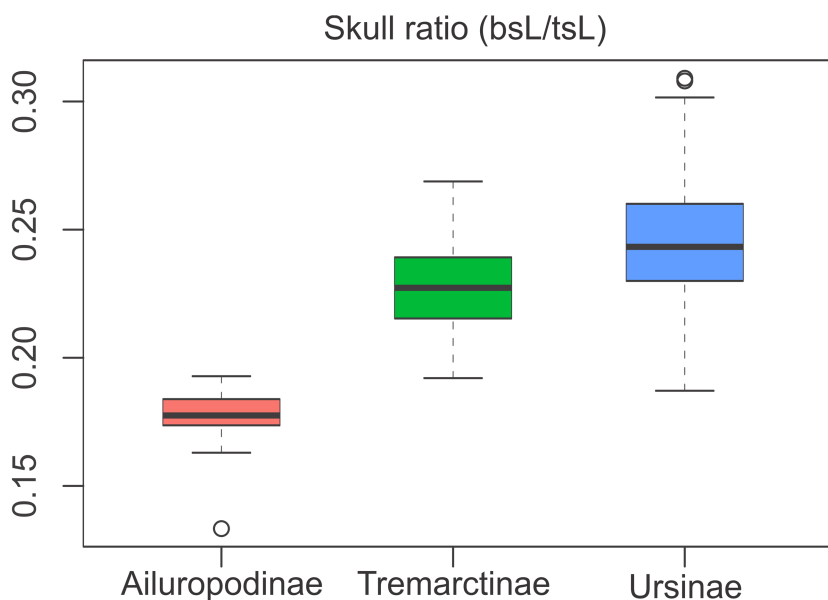
Figure 6 Boxplot of the skull ratio (bsL/tsL) per subfamilies where significant differences amongst them are observed. Boxes's floor and roof denote first and third quartile, respectively. Whiskers show 1.5 interquartile range, and blank circles are outliers.

contact anteriorly concave, otic region more expanded with larger tympanic bone, occipital condyles wider and posteriorly located, ventral margin of the foramen magnum also posteriorly located and foramen postglenoideum anteriorly located. In the current study, a high phylogenetic signal was also obtained in these principal nodes, showing that some ecological and biogeographic factors could be involved in the macroevolution of the braincase shape of ursids. However, this is not reflected in the size because ursids with similar basicranium shapes show different sizes and eating behaviours.

We observed that the node 'Tremarctinae+Ursinae' included some major lineages (e.g., *Ursus arctos* and *U. maritimus*) that inhabit open habitats (e.g., grasslands, savannas) and others in closed habitats (e.g., different types of forests; see Table S4). Also, those that live in closed habitats (e.g., black bears, *Helarctos malayanus*) are omnivore-hypocarnivore (feeding mainly on plant matter but incorporating insects and occasionally small mammals), small sized and live in tropical, subtropical or temperate climates (i.e., they do not rely on fat storage for winter). On the other hand, those bears that inhabit open habitats (i.e., *Ursus arctos*, *U. maritimus*) are omnivore–carnivore animals and sometimes feed on plants too, are larger in size and live (or lived in the case of extinct taxa, i.e., *Ar simus* and *A. angustidens*) under much more severe climates, so they present a larger motivation to gain fat during favourable seasons (see Table S4).

If we score and optimise open (red lines) versus closed (green lines) habitat preferences on the cladogram (Fig. 7), it can be seen that at the cladogenetic event that occurred on node 2 (when the Tremarctinae and Ursinae subfamilies differentiated), the preference for open habitats (Tremarctinae) or closed habitats (Ursinae) could have been a factor. These two
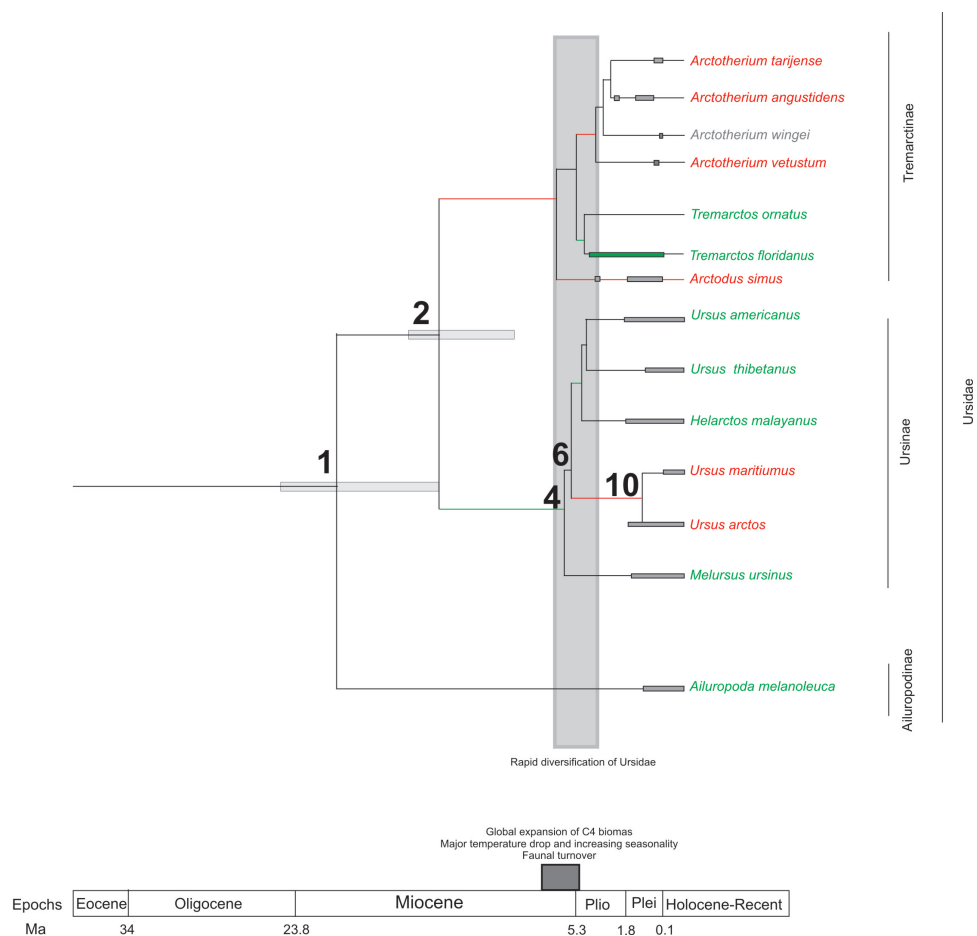
Figure 7 **Cladogram in which habitat preferences where scored and optimized.** Open habitat are in red lines, while closed habitats are in green lines (Modified from *Krause et al., 2008*).

clades may represent different solutions for balancing energy expenditure, intake, foraging time, fat accumulation and fitness, depending on food availability, foraging efficiency, body size and condition, as suggested by *Welch et al. (1997)* regarding the frugivory by bears. It is possible that the phylogenetic signal observed in the basicranium shape on node 2 would be related to an early differentiation of these two different evolutionary trends.

Compared with Ursinae, Tremarctinae shows a distinctive basicranium morphology characterised with a straight basioccipital–basiesphenoid contact; the basioccipital area is more expanded in relation to the otic region, which is located anteriorly with a wider mastoid process (PC2 also shows a high phylogenetic signal; Fig. 2). This configuration of the basicranium is practically conservative among Tremarctinae, independent of size variation (∼100 kg to ∼1,200 kg) and diet. Different proportions of the basicranium observed within Tremarctinae respective to the total length of the skull could be related to its diet (Fig. 6). Although all species exhibit almost the same basicranium configuration, the species that consumed higher amounts of animal items (e.g., scavengers such as *A. angustidens* and *Ar. simus*) present a smaller skull ratio and species with high amounts of

herbivore items (e.g., *T. floridanus* and *A. wingei*) present the higher skull ratios; however, those species (e.g., *A. vetustum* and *A. tarijense*) with an intermediate proportion of vegetal items in their diets showed intermediate values of skull ratios (Table S5). In this way, the high phylogenetical signal for the node Tremarctinae probably indicates that the general configuration of the basicranium in these bears was obtained early in their evolutionary history (which is in line with (*Krause et al., 2008*), who stated that Tremarctinae diverged about 12.4 to 15.6 Ma; Fig. 7).

The modifications in the skull of Ursidae could be the result of major climatic changes that occurred during the early cladogenesis of the largest bear clades; *Krause et al. (2008)*, see their Figs. 1 and 2) observed an explosive radiation of Ursidae at or just after the Mio-Pliocene boundary, suggesting that it was related to the paleoecological context of the Mio-Pliocene boundary, which had the following factors: (1) global increase in C4 biomass, where open wooded grassland habitats replaced the earlier, less seasonal woodland forest, resulting in habitat diversity reduction (*Ehleringer et al., 1991*; *Ehleringer, Cerling & Helliker, 1997*); (2) the Late Miocene carbon shift that resulted in a latitudinal gradient of C3/C4 grasses, with C3 grasses predominating in colder, more polar regions and C4 grasses predominating in temperate and tropical regions (*MacFadden, 2000*); (3) C4 biomass expanded in tropical to temperate regions; (4) major temperature drops came with an increase of seasonality; (5) terrestrial environments on all continents (except Antarctica) underwent major changes in fauna at the Mio-Pliocene boundary (60–80 genera of mammals were removed both in North America and Eurasia; *Savage & Russell, 1983*; *Web, 1983*; *Webb, 1984*; *Cerling, Ehleringer & Harris, 1998*); (6) the Plio-Pleistocene predator guild differed from all previous guilds in that it included a variety of carnivores with clear long-distance pursuit abilities. In this regard, massive predators were replaced by omnivorous bears and more specialised carnivores, such as felids and hyaenids (*Van Valkenburgh, 1999*).

These changes in habitat and food sources affected bears' ecology during the differentiation of the main clades. They became adaptable opportunists (e.g., *Peyton, 1980*; *Raine & Kansas, 1990*; *Wong, Servheen & Ambu, 2002*; *Hansen et al., 2010*; *Donohue, 2013*), and dietary versatility may have allowed ursids to persist during the dramatic habitat fluctuations of the Pleistocene and Holocene, favouring the wider distribution of the members of this family (*Krause et al., 2008*).

CONCLUDING REMARKS

Our results indicate that the variation of the basicranium shape (but not size) is significantly correlated with the topology of the cladogram, which depicts phylogenetic relationships. That is, the basicranium shape appears to be explained by a common heritage. The most significant nodes where phylogenetic autocorrelation of the basicranium shape was detected included basal differentiation of the major ursid lineages, indicating that cladogenesis of pandas, Ursinae and Tremarctinae was caused by evolutionary trends, and the resulting similarity among taxa analysed here could be explained by long-lasting influential factors. In this sense, early differentiation of Tremarctinae and Ursinae could be related to historical

events involving different environmental food preferences, which could be the factors that influenced the subsequent evolution of basicranium shape.

Our results of the basicranium/skull length ratios indicate that in Tremarctinae basicranium, size was not determined largely by phylogeny but rather by other factors such as adaptive responses to climatic changes and competition with other carnivores.

ACKNOWLEDGEMENTS

We want to thank Dr. Martín Ezcurra for his invaluable help with the optimisation of characters and the reviewers for their suggestions on early versions of this manuscript. We thank Melanie Canosa (University of Technology, Sydney) for her valuable and useful suggestions on an early version of this manuscript.

Funding

This work was partially supported by PICT 2016-2698 Préstamo BID. The funders had no role in study design, data collection and analysis, decision to publish, or preparation of the manuscript.

Grant Disclosures

The following grant information was disclosed by the authors:
PICT 2016-2698 Préstamo BID.

Competing Interests

The authors declare there are no competing interests.

Author Contributions

- María Eugenia Arnaudo conceived and designed the experiments, performed the experiments, analyzed the data, contributed reagents/materials/analysis tools, prepared figures and/or tables, approved the final draft.
- Néstor Toledo conceived and designed the experiments, performed the experiments, contributed reagents/materials/analysis tools, prepared figures and/or tables, approved the final draft.
- Leopoldo Soibelzon analyzed the data, authored or reviewed drafts of the paper, approved the final draft.
- Paula Bona conceived and designed the experiments, analyzed the data, contributed reagents/materials/analysis tools, authored or reviewed drafts of the paper, approved the final draft.

Data Availability

The raw data are available in the Supplemental Files.

PeerJ _______________

Supplemental Information

Supplemental information for this article can be found online at http://dx.doi.org/10.7717/peerj.6597#supplemental-information.

REFERENCES

Abouheif E. 1999. A method for testing the assumption of phylogenetic independence in comparative data. *Evolutionary Ecology Research* **1**:895–909.

Arnaudo ME, Fernandez Blanco MV. 2016. Estudio morfogeométrico del basicráneo de Ursidae (Carnivora, Mammalia). *Revista Ciencias Morfológicas* **18(2)**:1–10.

Baker WJ, Savolainen V, Asmussen-Lange CB, Chase MW, Dransfield J, Forest F, Madeline MH, Natalie WUh, Wilkinson M. 2009. Complete generic-level phylogenetic analyses of palms (Arecaceae) with comparisons of supertree and supermatrix approaches. *Systematic Biology* **58(2)**:240–256 DOI 10.1093/sysbio/syp021.

Bininda-Emonds OR. 2004. The evolution of supertrees. *Trends in Ecology & Evolution* **19(6)**:315–322 DOI 10.1016/j.tree.2004.03.015.

Cerling TE, Ehleringer JR, Harris JM. 1998. Carbon dioxide starvation, the development of C4 ecosystems, and mammalian evolution. *Philosophical Transactions of the Royal Society B: Biological Sciences* **353(1365)**:159–171 DOI 10.1098/rstb.1998.0198.

Davis DD. 1964. The giant panda. A morphological study of evolutionary mechanism. *Fieldiana, Zoology Memoirs* **3**:1–399.

Donohue SL. 2013. Using dental microwear textures to assess feeding ecology of extinct and extant bears. D Phil. Thesis, Vanderbilt University.

Dray S, Dufour AB. 2007. The ade4 package: implementing the duality diagram for ecologists. *Journal of Statistical Software* **22(4)**:1–20 DOI 10.18637/jss.v022.i04.

Dray S, Jombart T. 2008. Adephylo: exploratory analyses for the phylogenetic comparative method. *Bioinformatics* **26**:1907–1909 DOI 10.1093/bioinformatics/btq292.

Ehleringer JR, Cerling TE, Helliker BR. 1997. C4 photosynthesis, atmospheric CO2, and climate. *Oecologia* **112(3)**:285–299 DOI 10.1007/s004420050311.

Ehleringer JR, Sage RF, Flanagan LB, Pearcy RW. 1991. Climate change and the evolution of C4 photosynthesis. *Trends in Ecology & Evolution* **6(3)**:95–99 DOI 10.1016/0169-5347(91)90183-X.

García N, Santos E, Arsuaga JL, Carretero JM. 2007. Endocranial morphology of the *Ursus deningeri* Von Reichenau 1904 from the Sima de Los Huesos (Sierra de Atapuerca) Middle Pleistocene site. *Journal of Vertebrate Paleontology* **27(4)**:1007–1017 DOI 10.1671/0272-4634(2007)27[1007:EMOTUD]2.0.CO;2.

Garshelis DL. 2009. Familiy Ursidae (Bears). In: Wilson DE, Mittermeier RA, eds. *Handbook of the mammals of the world, volume 1: carnivores.* Barcelona: Lynx Edicions, 448–498.

Gittleman JL, Kot M. 1990. Adaptation: statistics and a null model for estimating phylogenetic effects. *Systematic Zoology* **39**:227–241 DOI 10.2307/2992183.

Goloboff PA, Catalano SA. 2016. TNT version 1.5, including a full implementation of phylogenetic morphometrics. *Cladistics* **32(3)**:221–238 DOI 10.1111/cla.12160.

Hansen RL, Carr MM, Apanavicius CJ, Jiang P, Bissell HA, Gocinski BL, Maury F, Himmelreich M, Beard S, Ouellette JR, Kouba AJ. 2010. Seasonal shifts in giant panda feeding behavior: relationships to bamboo plant part consumption. *Zoo Biology* **29**:470–483 DOI 10.1002/zoo.20280.

Harmon LJ, Weir JT, Brock CD, Glor RE, Challenger W. 2008. GEIGER: investigating evolutionary radiations. *Bioinformatics* **24**:129–131 DOI 10.1093/bioinformatics/btm538.

Harvey PH, Pagel MD. 1991. *The comparative method in evolutionary biology.* Oxford: Oxford University Press.

Hood CS. 2000. Geometric morphometric approaches to the study of sexual size dimorphism in mammals. *Hystrix* **11**:77–90 DOI 10.4404/hystrix-11.1-4137.

Hunt RMJ. 2001. Basicranial anatomy of the living linsangs *Prionodon* and *Poiana* (Mammalia, Carnivora, Viverridae), with comments on the early evolution of aeluroid carnivorans. *American Museum Novitates* **3330**:1–24 DOI 10.1206/0003-0082(2001)330<0001:BAOTLL>2.0.CO;2.

Jerison HJ. 1973. *Evolution of the brain and intelligence.* New York: Academic Press.

Jin C, Ciochon RL, Dong W, Hunt RM, Liu J, Jaeger M, Zhu Q. 2007. The first skull of the earliest giant panda. *Proceedings of the National Academy of Sciences of the United States of America* **104(26)**:10932–10937 DOI 10.1073/pnas.0704198104.

Juárez Casillas LA, Varas C. 2011. Genética evolutiva y molecular de la familia Ursidae: una revisión bibliográfica actualizada. *Therya* **2**:47–65 DOI 10.12933/therya-11-22.

Kamilar JM, Cooper N. 2013. Phylogenetic signal in primate behaviour, ecology and life history. *Philosophical Transactions of the Royal Society B* **368(1618)**:20120341 DOI 10.1098/rstb.2012.0341.

Kamilar JM, Muldoon KM. 2010. The climatic niche diversity of Malagasy primates: a phylogenetic perspective. *PLOS ONE* **5(6)**:e11073 DOI 10.1371/journal.pone.0011073.

Keck F, Rimet F, Bouchez A, Franc A. 2016. Phylosignal: an R package to measure, test, and explore the phylogenetic signal. *Ecology and Evolution* **6(9)**:2774–2780 DOI 10.1002/ece3.2051.

Koufos GD, Konidaris GE, Harvati K. 2017. Revisiting *Ursus etruscus* (Carnivora, Mammalia) from the Early Pleistocene of Greece with description of new material. *Quaternary International* **497**:222–239 DOI 10.1016/j.quaint.2017.09.043.

Krause J, Unger T, Noçon A, Malaspinas A, Kolokotronis S, Stiller M, Soibelzon L, Spriggs H, Dear PH, Briggs AW, Bray SCE, O'Brien SJ, Rabeder G, Matheus P, Cooper A, Slatkin M, Pääbo S, Hofreiter M. 2008. Mitochondrial genomes reveal an explosive radiation of extinct and extant bears near the Miocene-Pliocene Boundary. *BMC Evolutionary Biology* **8(220)**:1–12 DOI 10.1186/1471-2148-8-220.

Kumar V, Lammers F, Bidon T, Pfenninger M, Kolter L, Nilsson MA, Janke A. 2017. The evolutionary history of bears is characterized by gene flow across species. *Scientific Reports* **7**:46487 DOI 10.1038/srep46487.

Lieberman DE, Ross CF, Ravosa MJ. 2000. The primate cranial base: ontogeny, function, and integration. *American Journal of Physical Anthropology* **113(31)**:117–169 DOI 10.1002/1096-8644(2000)43:31+<117::AID-AJPA5>3.0.CO;2-I.

Losos JB. 2008. Phylogenetic niche conservatism, phylogenetic signal and the relationship between phylogenetic relatedness and ecological similarity among species. *Ecology Letters* **11**:995–1007 DOI 10.1111/j.1461-0248.2008.01229.x.

MacFadden BJ. 2000. Cenozoic mammalian herbivores from the Americas: reconstructing ancient diets and terrestrial communities. *Annual Review of Ecology and Systematics* **31(1)**:33–59 DOI 10.1146/annurev.ecolsys.31.1.33.

Maddison WP, Maddison DR. 2017. *Mesquite: a modular system for evolutionary analysis.* Version 3.31. *Available at* http://mesquiteproject.org.

Mitchell E, Tedford RH. 1973. The Elaliarctinae, A new group of extinct aquatic carnivore and a consideration of the origin of the Oteridae. *Bulletin of the American Museum of Natural History* **151**:201–284.

Mitchell KJ, Bray SC, Bover P, Soibelzon L, Schubert BW, Prevosti F, Prieto A, Martin F, Austin J, Cooper A. 2016. Ancient mitochondrial DNA reveals convergent evolution of giant short-faced bears (Tremarctinae) in North and South America. *Biology Letters* **12(4)**:20160062 DOI 10.1098/rsbl.2016.0062.

Molina-Venegas R, Rodríguez MÁ. 2017. Revisiting phylogenetic signal; strong or negligible impacts of polytomies and branch length information? *BMC Evolutionary Biology* **17(1)**:53 DOI 10.1186/s12862-017-0898-y.

Neff NA. 1987. The basicranial anatomy of the Nimravidae (Mammalia: Carnivora): character analyses and phylogenetic inferences. Ph.D. dissert, City University of New York, New York.

O'Brien SJ, Nash WG, Wildt DE, Bush ME, Benveniste RE. 1985. A molecular solution to the riddle of the giant panda's phylogeny. *Nature* **317**:140–144 DOI 10.1038/317140a0.

Ollier S, Couteron P, Chessell D. 2006. Orthonormal transform to decompose the variance of a life-history trait across a phylogenetic tree. *Biometrics* **62(2)**:471–477 DOI 10.1111/j.1541-0420.2005.00497.x.

Pagès M, Calvignac S, Klein C, Paris M, Hughes S, Hänni C. 2008. Combined analysis of fourteen nuclear genes refines the Ursidae phylogeny. *Molecular Phylogenetics and Evolution* **47(1)**:73–83 DOI 10.1016/j.ympev.2007.10.019.

Paradis E, Claude J, Strimmer K. 2004. APE: analyses of phylogenetics and evolution in R language. *Bioinformatics* **20(2)**:289–290 DOI 10.1093/bioinformatics/btg412.

Pavoine S, Ollier S, Pontier D, Chessel D. 2008. Testing for phylogenetic signal in phenotypic traits: new matrices of phylogenetic proximities. *Theoretical Population Biology* **73(1)**:79–91 DOI 10.1016/j.tpb.2007.10.001.

Peyton B. 1980. Ecology, distribution, and food habits of spectacled bears, *Tremarctos ornatus*, in Peru. *Journal of Mammalogy* **61**:639–652 DOI 10.2307/1380309.

R Core Team. 2018. R: a language and environment for statistical computing. Vienna: R Foundation for Statistical Computing. *Available at* https://www.R-project.org/.

Rabeder G, Pacher M, Withalm G. 2010. Early pleistocene bear remains from Deutsch-Altenburg (lower Austria). *Geologica Carpathica* **61(3)**:192.

Radinsky LB. 1969. Outlines of canid and felid brain evolution. *Annals of the New York Academy of Sciences* **167(1)**:277–288 DOI 10.1111/j.1749-6632.1969.tb20450.x.

Radinsky L. 1971. An example of parallelism in carnivore brain evolution. *Evolution* **25(3)**:518–522 DOI 10.2307/2407350.

Radinsky LB. 1973. Are stink badgers skunks? Implications of neuroanatomy for mustelid phylogeny. *Journal of Mammalogy* **54**:585–593 DOI 10.2307/1378960.

Radinsky L. 1974. The fossil evidence of anthropoid brain evolution. *American Journal of Physical Anthropology* **41(1)**:15–27 DOI 10.1002/ajpa.1330410104.

Raine RM, Kansas JL. 1990. Black bear seasonal food habits and distribution by elevation in Banff National Park, Alberta. *Bears: Their Biology and Management* **8**:297–304 DOI 10.2307/3872932.

Rasband WS. 2006. ImageJ. US National Institutes of Health, Bethesda, Maryland, USA, 1997–2016. *Available at https://imagej.nih.gov/ij/*.

Santos E, Garcia N, Carretero JM, Arsuaga JL, Tsoukala E. 2014. Endocranial traits of the Sima de los Huesos (Atapuerca, Spain) and Petralona (Chalkidiki, Greece) Middle Pleistocene ursids. Phylogenetic and biochronological implications. *Annales de Paleontologie* **100(4)**:297–309 DOI 10.1016/j.annpal.2014.02.002.

Savage DE, Russell DE. 1983. *Mammalian paleofaunas of the world*. vol. 432. London: Addison-Wesley.

Soibelzon LH. 2002. Los Ursidae (Carnivora, Fissipedia) fósiles de la República Argentina. In Aspectos Sistemáticos y Paleoecológicos. D. Phil. Thesis, Universidad Nacional de La Plata.

Soibelzon LH. 2004. Revisión sistemática de los Tremarctinae (Carnivora, Ursidae) fósiles de América del Sur. *Revista del Museo Argentino de Ciencias Naturales* **6(1)**:107–133.

Soibelzon LH, Schubert BW, Posadas PE. 2010. A new phylogenetic analysis of Tremarctinae bears. In: *VII simpósio brasileiro de paleontologia de vertebrados*. Río de Janeiro: Actas del VII Simposio Brasileiro de Paleontología de Vertebrados, pp. 1: 114.

Soibelzon LH, Tonni EP, Bond M. 2005. The fossil record of South American short-faced bears (Ursidae, Tremarctinae). *Journal of South American Earth Science* **20**:105–113 DOI 10.1016/j.jsames.2005.07.005.

Strait DS. 2001. Integration, phylogeny, and the hominid cranial base. *American Journal of Physical Anthropology* **114(4)**:273–297 DOI 10.1002/ajpa.1041.

Torres T. 1988. Osos (Mammalia, Carnivora, Ursidae) del Pleistoceno de la Península Ibérica. *Publicación Especial del Boletín Geológico y Minero, Instituto Geológico y Minero de España* **94**:1–316.

Trajano E, Ferrarezzi H. 1994. A fossil bear from northeastern Brazil, with a phylogenetic analysis of the South American extinct Tremarctinae (Ursidae). *Journal of Vertebrate Paleontology* **14**:552–561 DOI 10.1080/02724634.1995.10011577.

Turner HN. 1848. Observations relating to some of the foramina at the base of the skull in Mammalia; and on the classification of the Order Carnivora. *Proceedings of the Zoological Society of London* **1**:63–88.

Ubilla M, Perea D. 1999. Quaternary vertebrates of Uruguay: a biostratigraphic, biogeographic and climatic overview. *Quaternary of South America and Antarctic Peninsula* **12**:75–90.

Valkenburgh B. 1999. Major patterns in the history of carnivorous mammals. *Annual Review of Earth and Planetary Sciences* **27(1)**:463–493 DOI 10.1146/annurev.earth.27.1.463.

Wang X, Tedford RH. 1994. Basicranial anatomy and phylogeny of primitive canids and closely related miacids (Carnivora, Mammalia). *Dataset.* American Museum novitates; no. 3092. *Available at http://hdl.handle.net/2246/2841.*

Web SD. 1983. The rise and fall of the late Miocene ungulate fauna in North America. In: Nitecki 1, ed. *Coevolution.* Chicago: University of Chicago Press, 267–306.

Webb SD. 1984. Ten million years of mammal extinctions in North America. In: Martin PS, Klein RG, eds. *Quaternary extinctions: a prehistoric revolution.* Tucson: University of Arizona Press, 189–210.

Welch CA, Keay J, Kendall KC, Robbins CT. 1997. Constraints on frugivory by bears. *Ecology* **78(4)**:1105–1119 DOI 10.1890/0012-9658(1997)078[1105:COFBB]2.0.CO;2.

Wible JR. 1986. Transformations in the extracranial course of the internal carotid artery in mammalian phylogeny. *Journal of Vertebrate Paleontology* **6(4)**:313–325 DOI 10.1080/02724634.1986.10011628.

Wible JR. 1987. The eutherian stapedial artery: character analysis and implications for superordinal relationships. *Zoological Journal of the Linnean Society* **91**:107–135 DOI 10.1111/j.1096-3642.1987.tb01725.x.

Wible JR, Hopson J. 1993. In: Szalay FS, Novacek MJ, McKenna MC, eds. *Basicranial evidence for early mammal phylogeny.* New York: Springer-Verlag, 45–62.

Wilson DE, Reeder DM. 2005. *Mammal species of the world: a taxonomic and geographic reference (Vol. 1).* Baltimore: Johns Hopkins University Press.

Wong ST, Servheen CH, Ambu L. 2002. Food habits of malayan sun bears in lowland tropical forests of Borneo. *Ursus* **13**:127–136.

Wozencraft WC. 1989. The phylogeny of the recent Carnivora. In: Gittleman JL, ed. *Carnivore behavior, ecology, and evolution.* Ithaca: Cornell University Press, 495–535.